Materials Science in Semiconductor Processing 85 (2018) 98–105

Contents lists available at ScienceDirect

Materials Science in Semiconductor Processing

journal homepage: www.elsevier.com/locate/mssp

The investigation of current-conduction mechanisms (CCMs) in Au/(0.07Zn-PVA)/n-4H-SiC (MPS) Schottky diodes (SDs) by using (*I-V-T*) measurements

M. Hussein Al-Dharob[a,*], H. Elif Lapa[b], A. Kökce[b], A. Faruk Özdemir[b], D. Ali Aldemir[b], Ş. Altındal[c]

[a] Graduate School of Natural and Applied Sciences, Süleyman Demirel University, Isparta, Turkey
[b] Department of Physics, Faculty of Arts and Sciences, Süleyman Demirel University, Isparta, Turkey
[c] Department of Physics, Faculty of Sciences, Gazi University, Ankara, Turkey

ARTICLE INFO

Keywords:
Au/(Zn-PVA)/n-4H-SiC (MPS) type Schottky diodes
Possible current-conduction mechanism
Barrier inhomogeneities
Double Gaussian distribution (DGD) of barrier height

ABSTRACT

The semi-logarithmic forward bias *I-V* plots of the Au/(0.07Zn-PVA)/n-4H-SiC (MPS) type SBDs showed double exponential behavior therefore these plots revealed two distinct linear regions which correspond to low (0.05 V ≤ 0.4 V) and moderate voltage regions (0.4 ≤ V ≤ 0.8 V) (LBR and MBR), respectively, for each temperature level. It was observed that the value of ideality factor (n) decreased with increasing temperature whereas opposite behavior occurred for zero-bias barrier height (Φ_{B0}). The behavior of nkT/q vs kT/q plot for MBR indicated that a combination of thermionic field emission (TFE) and field emission (FE) mechanisms, i.e. the tunneling mechanism, may be dominant especially at low temperatures. In order to explain such unexpected behavior of the conduction mechanism; Φ_{B0} vs n, Φ_{B0} vs $q/2kT$ and $(n^{-1} - 1)$ vs $q/2kT$ plots were drawn to obtain an evidence of a Gaussian distribution (GD) of the barrier heights (BHs) and all of them revealed two linear regions for both LBR and MBR. The conventional Richardson plot was modified by using the obtained standard deviation (σ_{so}) of BH from Φ_{B0} vs $q/2kT$ plots for two bias regions. Thus, the mean BH ($\bar{\Phi}_{B0}$) and effective Richardson constant (A^*) values for LBR were calculated from the slope and intercept of the modified Richardson plots as 0.730 eV, 114.12 A cm^{-2} K^{-2} at low temperature range (100 ≤ T ≤ 200 K) and 1.304 eV, 97.33 A cm^{-2} K^{-2} at high temperature range (200 ≤ T ≤ 320 K), respectively. These values for MBR were found as 0.687 eV, 144.97 A cm^{-2} K^{-2} at low temperature range and 1.165 eV, 122.11 A cm^{-2} K^{-2} at high temperature range, respectively. It is clear that the values of A^* for MBR at low temperatures are closer to 146 A cm^{-2} K^{-2} which represents the theoretical value of for n-4H-SiC. As a result, the current conduction mechanisms (CCM) in Au/(0.07Zn-PVA)/n-4H-SiC (MPS) SD can be successfully explained by thermionic emission (TE) mechanism with the double GD of BHs.

1. Introduction

It is a necessary demand to devolve the cost-effective devices with high performance instead of conventional metal-semiconductor (MS) and metal-insulator-semiconductor (MIS) structures. It is believed that a controlling of barrier height (BH), a decrease in series resistance (R_s), and an increase in rectifying ratio can be possible with the usage of a dielectric layer with high dielectric constant between a metal and semiconductor. Therefore, recently, many researchers have focused on the fabrication of the metal-semiconductor (MS) type Schottky diodes with a doped interfacial polymer layer instead of traditional or conventional insulator layer such as SiO_2 and SnO_2 due to low cost, low weight, flexibility and easy processes of polymers [1–6]. For such an application, poly(vinyl alcohol) (PVA) is one of the most significant polymeric material due to its physical and chemical properties such as water-soluble, semi-crystalline structures, wide range crystallinity, and poor conductivity. Besides these properties, its good charge storage capacity and high dielectric strength arising from its hydrogen formation and OH group make it attractive material for MIS capacitors [3–5]. Furthermore, the polymer conductivity is based on extensive interactions of polymer chains via hydrogen bonding between the doping metals and the hydroxyl groups.

On the other hand, many researchers are also interested in the temperature dependence of both n and BH [7–16]. The analysis of the *I-V* characteristics of these diodes based on TE mechanism usually reveals an abnormal increase in Φ_{B0} and a decrease in the n with an increase in

* Corresponding author.

https://doi.org/10.1016/j.mssp.2018.05.032
Received 23 December 2017; Received in revised form 23 May 2018; Accepted 26 May 2018
Available online 20 June 2018

the temperature. Such behavior of n and Φ_{B0} with temperature leads to non-linearity in the Richardson plots of ($\ln(I_0/T^2)$ vs q/kT) and yield very low experimental value of Richardson constant (A^*) compared with its theoretical value of it [10–16]. Therefore, such behavior of Φ_{B0}, n and the non-linearity behavior of Richardson plots especially at low temperatures have been successfully explained by the basis of TE mechanism with a GD of BHs rather than the other CCMs [7–16].

Silicon carbide type (4H-SiC) semiconductor is the most studied promising inorganic material due to its chemical, mechanical and physical properties such as chemical inertness, hardness, high thermal conductivity, high mobility, abrasive wear resistance, wide bandgap (E_g), and high-power. In addition, it has the ability to form silicon dioxide (SiO_2) as a native oxide layer. Therefore, SiC has been developed as a high-power, high-temperature semiconductor electronics device. The main application area of devices includes wireless technologies, high sensitive switches for harsh environment sensors and automotive applications [17,18]. The charge carrier transport from electrodes into polymer material constitutes one important factor of performance for MS type structures [19–21]. PVA is also an interesting artificial polymer due to its solubilized crystalline structure polymer in water and can be acquired industrially by the alkaline hydrolysis of solutions of poly (vinyl acetate) (PVA) [22–27]. PVA has also very high dielectric permittivity, good charge storage capacity and dopant-dependent electrical and optical properties; furthermore, it was used widely in alteration of duct and articular cartilage [28–31]. The main advantage of polymer layer, which make it an important parameter in different applications, is its high clarity, lack of charge density properties, excellent durability and thermal stability in wide temperature range. Polymers have various physical and chemical properties, including microstructural, optical, electrical and thermal properties and they depend on the chemical nature of the dopant and the process of the interaction with the host polymer [32,36]. When PVA is doped with transition elements such as Zn, Co, Ni with different ratios, its conductivity is considerably increased and it behaves like a conductive polymer [34,35]. Thus, the microstructural property of the polymer in new form constitutes a new kind of conductive polymeric material with a lower leakage current and this improves the electrical and dielectric properties of PVA [28–35].

In order to get more information on the CCMs and formation of BH at M/S interface, the electrical characterization must be evaluated in a wide range of temperature and voltage [36–42]. *I-V* measurements taken only at a single temperature level cannot supply detailed information on both CCMs and BH. Especially at low temperatures, the CCM is quite complex and difficult [42–47]. The determination of CCMs especially at low or moderate temperatures becomes more complicated and the investigation of forward biases *I-V-T* characteristics in these devices based on *TE* theory generally yields an unknown increase in Φ_{B0} and a decrease in n with increasing temperature [28–34]. Both Tung [12] and Schmitsdrof et al. [49] observed the non-uniformity (inhomogeneity) of BH at M/S interface. Moreover, spot density in inhomogeneity pattern can be obtained to explain high values of n and low values of BH on smaller local spots with lower *BH* than a mean *BH* at junction. Therefore, at low temperatures, current flows through these patches or lower BHs which are located around mean BH and this yields a large value of n [28,36–40,48–52]. According to Song et al. [13], the barrier in-homogeneities may happen in the composition of interfacial layer, its thickness and interfacial charges.

The main aim of this study is to fabricate Au/(0.07Zn-PVA)/n-4H-SiC (MPS) type SDs instead of traditional MIS type and achieve a detailed review on the CCMs and the formation of BH as function of temperature and voltage. For this purpose, the forward bias *I-V* characteristics of these SDs are performed in the temperature domain of (100–320 K) by 20 K steps. In this way, we tried to clarify the origin of high values of n and positive temperature coefficient of BH especially below room temperature. Because, at or above room temperature, CCM is usually governed by TE theory and the value of n is closer to unity. Our experimental results show high values of n and low values of BH especially at low temperatures that can be explained successfully by applying the DGD of BHs around a mean value of BH.

2. Experimental procedure

The Au/(0.07Zn-PVA)/n-4H-SiC (MPS) SDs were manufactured on the n-type 4H-SiC wafer with (0001) orientation, 250 μm thickness, and 7.07×10^{17} cm^{-3} concentration of the donor atoms. Firstly, n-4H-SiC wafer was cleaned in the ultrasonic bath by using various chemical solvents and then dried by dry nitrogen (N_2) gas. After cleaning processes, immediately, n-4H-SiC wafer was transferred to vacuum chamber and then high-purity (99.999%) of gold (Au) with 1500 Å was thermally evaporated on the back side of it at about 10^{-6} Torr. In order to perform high quality or low resistivity ohmic contact, (n-4H-SiC)/Au was annealed at 550 °C in the nitrogen ambient for 5 min.

Polyvinyl alcohol (PVA-Mw 130,000 g/mol, from Sigma Aldrich) was used as the polymeric precursor. 0.1 g of zinc acetate was mixed with 0.9 g of PVA, molecular weight = 72,000 and 9 ml of deionized water. After vigorous stirring for 2 h at 50 °C, a viscous solution of PVA:Zn acetates was obtained. Using a peristaltic syringe pump, the precursor solution was delivered to a metal needle syringe (10 ml) with an inner diameter of 0.9 mm at a constant flow rate of 0.02 ml/h. The needle was connected to a high voltage power supply and positioned vertically on a clamp. A piece of flat Al foil was placed 18 cm below the tip of the needle to collect the nanofibers and then the n-type 4H-SiC wafer was placed on the Al foil. Upon applying a high voltage of 20 kV on the needle, a fluid jet was ejected from the tip. In order to insert a thin polymer film between Au and n-4H-SiC as interfacial layer, after the formation of ohmic contact, the prepared (0.07Zn-doped PVA) solvent was deposited on the n-4H-SiC wafer by using electrospinning method. The thickness of polymer layer was estimated as 50 nm thickness. Finally, high-purity Au dots/rectifier contact with 1 mm radius were also thermal grown on the (0.07Zn-doped PVA) polymer. The thickness of the layers of the structure was observed by using a quartz crystal thickness monitor. In order perform I-V measurements, samples were pasted on a copper holder using a silver paste and then thin silver coated Cu wires were used to make the electrical contacts to the upper electrodes.

The forward bias *I-V* measurements were carried out in the Janis VPF-475 cryostat in the temperature range of (100–320 K) using a Lake Shore model 321 auto-tuning temperature controllers with sensitivity better than ± 0.1 K. All these measurements were carried out with the help of a microcomputer through an IEEE-488 ac/dc converter card. Further details of the fabrication processes of the samples can be found in our previous study [53]. The schematic representation of the electrospinning system and the schematic diagram of the fabricated MPS type SDs were given in Fig. 1(a) and (b), respectively.

Temperature dependent *I-V* measurements were performed by the use of a Keithley 2400 I-V source-meter in the Janis vpf-475 cryostat at about 10^{-3} Torr. The sample temperature was always watched by using a Lake Shore model 321 auto-tuning temperature controllers with sensitivity better than ± 0.1 K.

3. Results and discussion

The semi-logarithmic forward bias *I-V* characteristics of the Au/(0.07Zn-PVA)/n-4H-SiC (MPS) SD was given in Fig. 2 for various temperatures. As it is clearly seen, the ln*I vs V* plots have two distinct linear regions with different slopes for each temperature level. These two linear regimes represent the low bias region (LBR), 0.05 V ≤ 0.4 V, and moderate bias region (MBR), 0.4 ≤ V ≤ 0.8 V, respectively. Such behavior of ln*I* vs *V* plots is known as double-exponential or two parallel diodes model with different BH and resistance. After the second linear region, ln*I* vs *V* plot deviates from linearity because of the existence of series resistance (R_s) and interfacial layer. For MS type SDs with and without interfacial layer such as insulator or polymer (MIS or

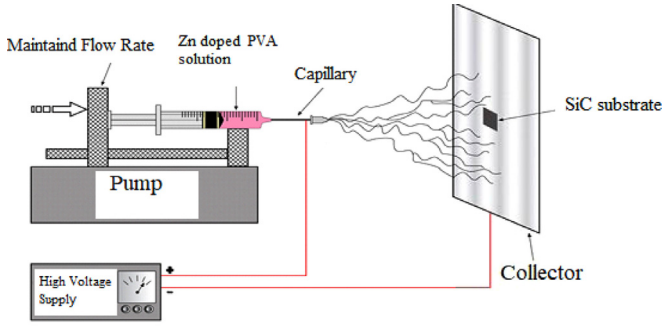

(a) The schematic representation of the electro-spinning system.

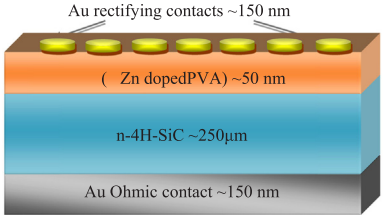

(b). The schematic diagram of the Au/(0.07Zn-PVA)/n-4H-SiC (MPS) SDs.

Fig. 1. (a) The schematic representation of the electro-spinning system. (b). The schematic diagram of the Au/(0.07Zn-PVA)/n-4H-SiC (MPS) SDs.

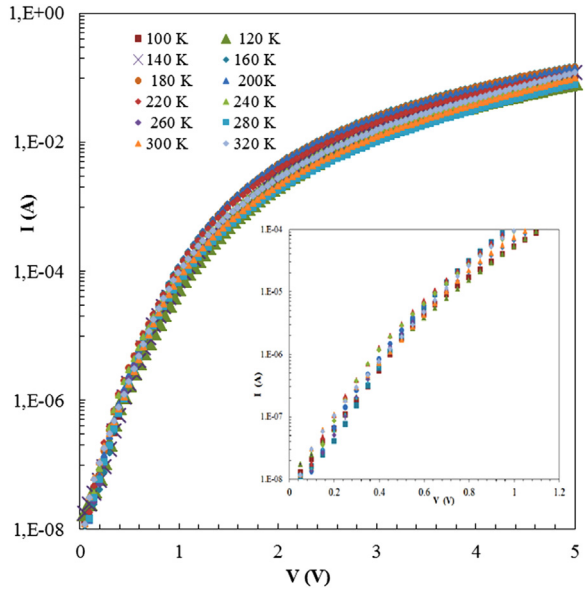

Fig. 2. The forward semi-logarithmic *I-V*-T characteristics of the Au/(Zn-PVA)/n-4H-SiC (MPS) type SD at various temperatures.

MPS), the relation between forward bias I and V based on *TE* theory ($V \geq 3kT/q$) can be expressed as [48–54]:

$$I = AA^{*}T^{2}\exp\left(-\frac{q}{kT}\Phi_{Bo}\right)\left[\exp\left(\frac{q(V-IR_{s})}{nkT}\right)-1\right] \quad (1)$$

The part in front of the square brackets in Eq. (1) corresponds to reverse-bias saturation current (I_o) and it is obtained from the interception of the linear part of ln*I-V* plot at zero voltage, Φ_{Bo} is the zero-bias barrier height, V is the applied voltage drop across the diode, A is the rectifier contact/diode area (0.0314 cm^2), A^* is the effective Richardson constant (146 A cm^{-2} K^{-2} for n-type 4H-SiC), the term of IR_s is the voltage drop across the R_s and others are well known quantities in the literature

Thus, the value of Φ_{Bo} can be obtained from Eq. (1) by using the values of I_o and rectifier contact area (A) of the diode for each temperature level:

$$\Phi_{Bo} = \frac{kT}{q}Ln\left(\frac{AA^{*}T^{2}}{I_{0}}\right) \quad (2)$$

The value of n of the SDs are also important since n is a decisive parameter that effect on the diode performance/quality by controlling on the charge transportation through interfaces and it can also be calculated from the slope of the linear part of the ln*I-V* plot as [48–53]:

$$n = \frac{q}{kT}\left(\frac{dV}{d(\ln I)}\right) \quad (3)$$

Thus these values of three main parameters (I_o, n and Φ_{Bo}) of Au/(0.07Zn-PVA)/n-4H-SiC (MPS) type SD for both at the LBR and MBR were obtained as function of temperature and tabulated in Table 1. As can be seen in Table 1, all these parameters are strong functions of temperature and they changed from 7.70 × 10^{-9} A, 10.99, 0.24 eV (at 100 K) to 1.68 × 10^{-8} A, 3.08 and 0.830 eV (at 320 K) for LBR. These parameters for MBR changed from 2.25 × 10^{-9} A, 13.31, 0.252 eV (at 100 K) to 9.89 × 10^{-8} A, 4.15 and 0.767 eV (at 320 K), respectively. In order to explore the effect of temperature of n and Φ_{Bo} of the MPS SD, the n and Φ_{Bo} versus T plots both for the LBR and MBR are shown in Fig. 3(a) and (b), respectively.

As can be seen in Table 1 and Fig. 3, while the value of n increases with decreasing temperature Φ_{BO} decreases. This change in the Φ_{BO} with temperature both for low and moderate voltages is in agreement with negative temperature of forbidden band-gap of semiconductor (E_g) or BH for and ideal SD. However, the obtained high values of n especially at low temperatures may be partly explained by the presence of interfacial (Zn-doped PVA) layer, a special density distribution of N_{ss} at interlayer/semiconductor interface and the dominant conduction by interface recombination, but main reason/origin of them is the barrier inhomogeneities at M/S interface [28,35–38,47–50]. As seen in Fig. 3(a) and (b), as temperature increases, the values of Φ_{BO} increase and almost exponential decrease is observed in the values of n. This behavior of Φ_{BO} with temperature and high values of n show that there is a deviation from the standard/pure TE theory especially at low temperature. Because, it is expected that the value of n must be unity or close to unity near the room temperature based on pure or standard TE theory, and furthermore the value of Φ_{BO} must be increased with decreasing temperature like the forbidden band gap (E_g) of the semiconductor.

These observed lower values of Φ_{BO} at low temperatures can be attributed to that the charges at low temperatures are able to climb the minimal barriers or patches and so current transport will be controlled by the charges that flow through these lower BHs or patches and this leads to an increase in current or n [35–38]. When temperature reaches a sufficient level, more and more charge carriers gain enough thermal energy to climb the elevated barriers. Therefore, it can be said that the obtained values of Φ_{BO} do not represent the mean BHs, instead they represent the apparent BHs ($\Phi_{ap.}$) for each temperature and voltage. At low temperatures the possible CCMs become more complicated and considerably different from the mechanisms at or above temperatures. Therefore the apparent BH at low temperatures is low because of the pinch-off/patches around the mean value of BH between metal and semiconductor [37,38,41,44]. Usually, the energy band-diagram of the MS type diode with barrier in-homogeneities is represented at Fig. 4 [12,15]. It is clear that the charges at low temperatures can easily pass through low barriers/patches and so leads to an increase in current or ideality factor (n) [12–15]. In other words, the charge carriers do not have enough energy to pass through the top of barrier at low temperatures, but they can pass through the lower barriers or patches at around mean barrier height. Therefore, the obtained values of Φ_{BO} do not correspond to the mean BHs, instead they correspond to the

Table 1
The experimental values of I_o, n and Φ_{BO} obtained from the forward bias I-V data for LBR and MBR for the Au/(0.07Zn-PVA)/n-4H-SiC (MPS) type SD for various temperatures.

LBR (Low Bias Region)				*MBR (Moderate Bias Region)*			
T (K)	I_0 (A)	n	Φ_{B0} (eV)	T (K)	I_0 (A)	n	Φ_{B0} (eV)
100	7.70×10^{-9}	10.99	0.24	100	2.25×10^{-9}	13.31	0.252
120	7.00×10^{-9}	8.55	0.29	120	3.75×10^{-9}	11.25	0.301
140	1.00×10^{-9}	7.40	0.34	140	8.30×10^{-9}	9.74	0.346
160	1.80×10^{-9}	6.039	0.40	160	9.20×10^{-9}	8.45	0.397
180	2.30×10^{-9}	4.529	0.47	180	1.52×10^{-8}	7.45	0.443
200	3.0×10^{-9}	3.99	0.52	200	2.09×10^{-8}	6.73	0.490
220	3.05×10^{-9}	3.63	0.57	220	3.42×10^{-8}	6.18	0.533
240	3.10×10^{-9}	3.42	0.63	240	3.50×10^{-8}	5.70	0.585
260	3.50×10^{-9}	3.29	0.69	260	4.39×10^{-8}	5.09	0.632
280	5.00×10^{-9}	3.27	0.74	280	5.85×10^{-8}	4.63	0.678
300	7.21×10^{-9}	3.24	0.77	300	7.06×10^{-8}	4.34	0.725
320	1.68×10^{-8}	3.08	0.83	320	9.89×10^{-8}	4.15	0.767

apparent BHs ($\Phi ap.$) for each temperature and voltage.

Another important electrical parameter of the Au/(0.07Zn-PVA)/n-4H-SiC (MPS) type SD is series resistance (R_s) which considerably influences the forward bias *I-V* characteristics at enough high forward voltages. There are various methods reported in the literature for the estimation of the R_s from the forward bias I-V data, but the simplest and most accurate and reliable one is the Ohm's law ($R_i = dV_i/dI_i$) which also prevents time consumption through its easy and quick application. Thus calculated resistance value at the sufficient high forward voltages simply corresponds to R_s Therefore, in this study, the voltage dependent values of resistance (R_i) were calculated using Ohm's Law ($R_i = dV_i/dI_i$) for five different temperature levels by 60 K steps and shown in Fig. 5. As shown in Fig. 5, at sufficiently high forward biases, the plots of R_i become almost constant and reveal the real value of R_s. As can be seen in Fig. 5, the value of R_s decreases with increasing temperature and it was found as 27.40 Ω, at 100 K and 20.78 Ω at 320 K, respectively. The low value of R_s can be accomplished by rather having low SBH at M/S interface or by increase tunneling through the BH by using heavily doped semiconductor ($\geq 10^{17}$ cm^{-3}) [44,56]. Usually, the existence of R_s may be originated from different sources which are the ohmic back and front Schottky/rectifier contacts, the contact of the wire to the gate probe, the resistivity of the bulk semiconductor, impurities/dislocations and random doping distribution in the semiconductor [43,55].

The increase in n and decrease in Φ_{BO} with decreasing temperature are a clear evidence of the deviation from the standard TE theory. This suggests that the tunneling (thermionic field emission (TFE) and FE mechanisms/theories) perhaps deserve consideration [1–8,47–52]. It is well known that the requirement of FE and TFE mechanisms is the change in the tunneling current parameter E_o ($= nkT/q$) as a function of temperature as [38,51,52,57]:

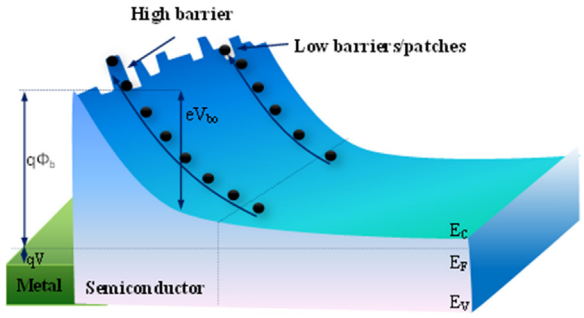

Fig. 4. A band diagram of the structure cross of the metal-semiconductor diode/structure.

$$I = I_{tun}\left[\exp\left(\frac{q(V - IR_s)}{E_o}\right) - 1\right] \tag{4}$$

with

$$n_{tun} = \frac{E_{oo}}{kT}\coth\left(\frac{E_{oo}}{kT}\right) = \frac{E_o}{kT}, \tag{5}$$

and

$$E_{oo} = \frac{h}{4\pi}\left(\frac{N_D}{m_e{}^*\varepsilon_s}\right)^{1/2} \tag{6}$$

where $m_e{}^*$ ($= 0.2m_o$) is effective mass of electron, m_o is the rest of electron mass and ε_s is the permittivity semiconductor ($= 9.7$ for 4H-SiC), ε_o ($= 8.85 \times 10^{-12}$ F/m) is the permittivity of the vacuum and N_D is the concentrations of doping donor atoms that was used in this study is about 7.07×10^{23} m^{-3}. By using Eq. (6), the theoretical value of E_{oo}

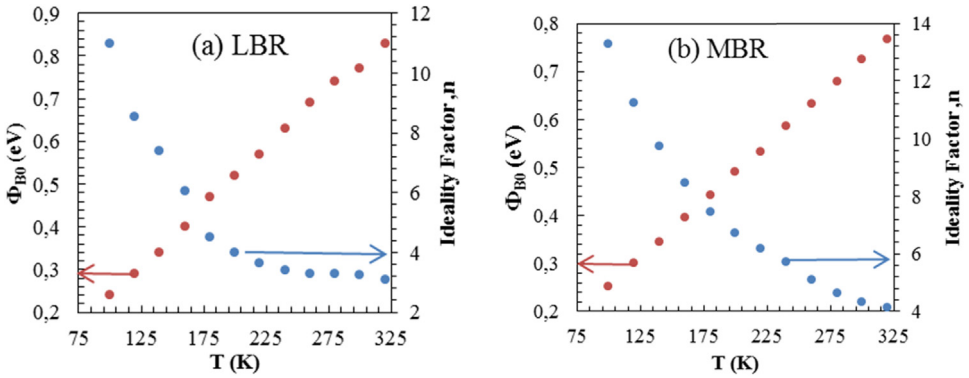

Fig. 3. The effect of temperature on n and Φ_{Bo} of the Au/(0.07Zn-PVA)/n-4H-SiC (MPS) type SD (a) for LBR and (b) for MBR, respectively.

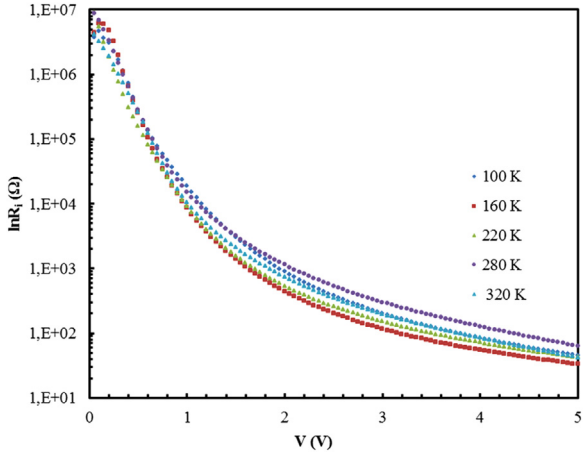

Fig. 5. The R_i *vs* V plot for the Au/(0.07Zn-PVA)/n-4H-SiC (MPS) type SD for various temperature by 60 K steps.

was calculated as 16.66 meV for room temperature. But, TFE should be valid or dominant when $E_{oo} \approx kT/q$; the TE is dominant if $E_{oo} \ll kT/q$ and the FE is dominant if $E_{oo} \gg kT/q$. Furthermore, if the FE is dominant, then the E_o or n.T must be almost constant for each temperature or independent of temperature [56,58,59] and in this case, E_o is equal to E_{oo}. Fig. 6(a, b) shows $E_{oo}(= nkT/q)$ vs kT/q plots of the Au/(0.07Zn-PVA)/n-4H-SiC (MPS) type SD in the temperature domain of 100–320 K for LBR and MBR, respectively. Using the data in Fig. 6, the value of E_o was found as 89.5 meV for LBR and 118.6 meV for MBR. It is clear that the experimental values of these parameters are considerably higher than the theoretical values of E_{oo} (16.66 meV). In other words, the evidence of T_0 effect can be obtained from nkT/q vs kT/q plot, also the fitting of the temperature dependence of ideality factor with Eq. (5) as shown in Fig. 6 can be explained by the effect of tunneling on the carrier transport across the BH. Thus, it can be said that the TFE and FE mechanism, both, are possible CCMs especially at low temperatures rather than TE theory.

On the other hand, it is difficult to clarify such behavior of high values of n especially due to low temperatures and positive temperature coefficient of BH by only TFE and FE theories. Therefore, we tried to clarify this non-ideal behavior of the forward-bias *I-V* characteristics in Au/(0.07Zn-PVA)/n-4H-SiC (MPS) type SD according to the basis of a TE mechanism with a Gaussian distribution (GD) of the BHs [47–52]. Usually, there are three basic evidences for the GD of BH which are Φ_{Bo} vs n, Φ_{Bo} vs $q/2kT$ and $(n^{-1} - 1)$ vs $q/2kT$ plots. For this purpose, these figures were drawn to obtain an evidence of GD of the BHs and they are represented in Figs. 7(a, b), 8(a, b) and 9(a, b) both for LBR and MBR, respectively.

Mönch [8] applied Tung's theoretical approach and they found a good linear correlation between Φ_{B0} and n which confirmed that the lateral in-homogeneities of the BHs between metal and semiconductor. Thus, the Φ_{B0} vs n plot to/for $n = 1$ should be given a homogeneous BH. As can be clearly seen in Fig. 7(a, b), Φ_{B0} vs n plots for both low (100–200 K) and high temperature (220–320 K) regimes have two distinctive linear regions with different slopes. Such behaviors of Φ_{B0} vs n plots for two temperature regimes are evidence to the lateral in-homogeneities of the BHs at M/S interface. The extrapolation of the results of Φ_{B0} vs n plot (Fig. 7a) in LBR, have given the mean values of BH ($\overline{\Phi}_{Bo}$) as 0.615 eV (at LTR) and 1.638 eV (at HTR), respectively, for $n = 1$ case. Similarly, they are obtained as 0.673 eV and 1.087 eV, respectively, for MBR. These experimental results offer the decrease in Φ_{Bo} and increase in n may be caused by the BH in-homogeneities at M/S interface.

According to the GD model recommended by Werner and Güttler [14], the total current through these patches or lower barriers at around mean BH for the forward bias can be expressed as:

$$I(V) = \int_{-\infty}^{+\infty} I(\Phi_B, V) P(\Phi_B) d\Phi \tag{7}$$

In Eq. (7), the $I(\Phi_B,V)$ is the current at a bias voltage for a BH based on the ideal TE-diffusion (TE-D) theory and $P(\Phi_B)$ is the normalized distribution function which detect the probability of accuracy for BH. Since, carrying out this integration in domain of -∞ to + ∞, one can calculate the current $I(V)$ through a barrier at a forward bias voltage as:

$$I(V) = AA^*T^2 \exp\left[-\frac{q}{kT}\left(\bar{\Phi}_{B0} - \frac{q\sigma_o^2}{2kT}\right)\right]\exp\left(\frac{qV}{n_{ap}kT}\right)\left[1 - \exp\left(-\frac{q(V - IR_s)}{kT}\right)\right] \tag{8}$$

Thus, the GD of the BH with a mean BH ($\overline{\Phi}_{Bo}$) and standard deviation (σ_o or σ_{so}) can be calculated by the following equation:

$$\Phi_{ap} = \overline{\Phi}_{Bo}(T = 0) - \frac{q\sigma_{so}^2}{2kT} \tag{9}$$

The other observed variation in the n with temperature in the model can be written as:

$$\left(\frac{1}{n_{ap}} - 1\right) = \rho_2 - \frac{q\rho_3}{2kT} \tag{10}$$

where ρ_2 and ρ_3 are the voltage coefficients, and n_{ap} is the apparent or measured value of n. As seen in Fig. 8(a, b), the Φ_{ap} vs $q/2kT$ plot for both LBR and MBR has also obvious two linear parts for LTR and HTR. Both the values of $\overline{\Phi}_{Bo}$ and σ_{so} can be calculated from the interception point of the Φ_{B0} axis and slope of this plot, respectively. Thus the intercept and slope of these linear parts for LBR have been two sets of

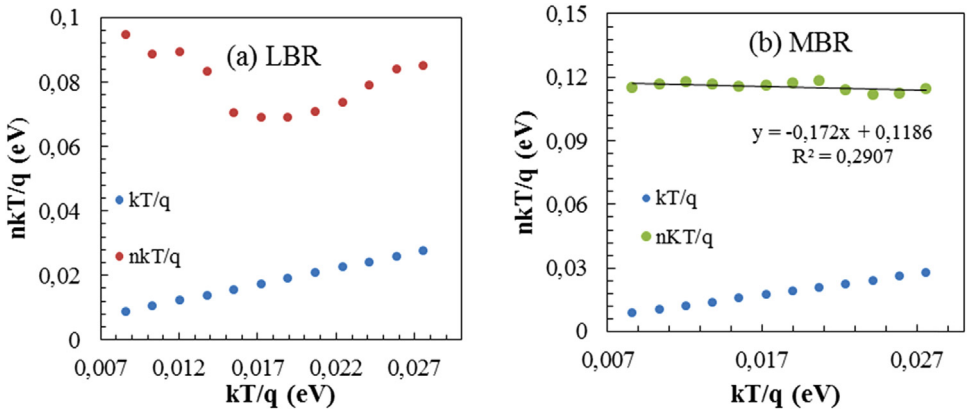

Fig. 6. The plots of nkT/q vs kT/q for Au/(0.07Zn-PVA)/n-4H-SiC (MPS) type SD for (a) LBR and (b)MBR, respectively.

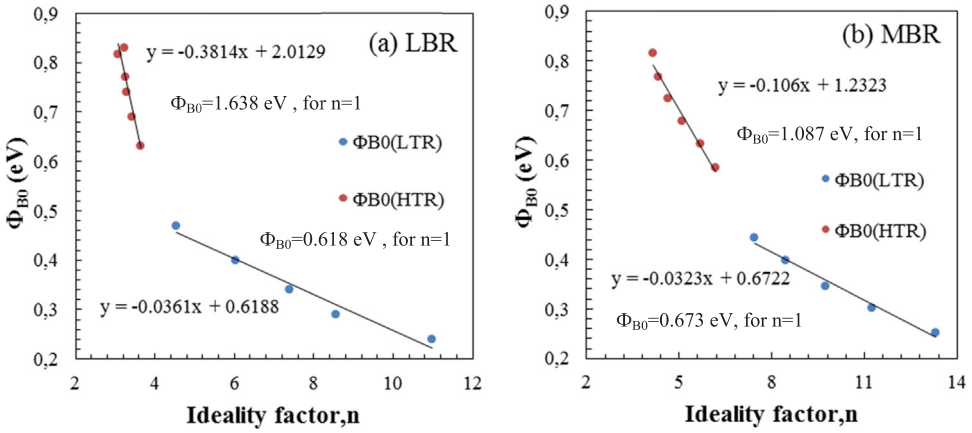

Fig. 7. Φ_{B0}-n plots for Au/(0.07Zn-PVA)/n-4H-SiC SD for (a) LBR and (b) MBR.

values of Φ_{B0} and σ_{so} as 0.0719 eV and 0.0086 V for LTR, and as 1.27 eV and 0.024 V for the HTR, respectively. In addition, these values for MBR were calculated as 0.663 eV and 0.0073 V for the LTR, and as 1.262 eV and 0.025 V for the HTR, respectively.

In Eqs. (9) and (10), it is prospective that the adjusted values of $\overline{\Phi}_{Bo}$ and σ_{so} depend on applied bias voltage linearly by the equations $\Phi_B = \overline{\Phi}_{Bo} + \rho_2 V$ and $\sigma = \sigma_{so} + \rho_3 V$. Usually, the value of σ_{so} is independent of temperature so that it can be neglected low. In order to calculate the values of voltage deformation coefficients ρ_2 and ρ_3, $(n_{ap}^{-1} - 1)$ *vs* $q/2kT$ plots for LBR and MBR were also drawn and given in the Fig. 9(a) and (b), respectively. As shown in Fig. 9(a, b), the $(n_{ap}^{-1} - 1)$ *vs* $q/2kT$ plot must also have different characteristics in the low and high temperature ranges (LTR, HTR) due to containing DG distribution of BHs at M/S interface. Thus, both the values of ρ_2 and ρ_3 are calculated from the intercepts and slope of the experimental $(n_{ap}^{-1} - 1)$ vs $q/2kT$ plots both for LBR and MBR. These values are found for LBR as − 0.0054 V, − 0.6175 V for LTR and as − 0.0052 V, − 0.5845 V for HTR, respectively. Similarly, for the MBR these values are also found as − 0.0025 V, − 0.7866 V for LTR and as − 0.0101 V, − 0.5766 V for HTR, respectively.

According to obtained experimental results/characterization above, both the inhomogeneity and potential variation in the BH dramatically affect the forward-bias *I-V* characteristics especially at low temperatures. So now, the classical Richardson/Arrhenius plot can be adjusted by combining Eqs. (1) and (2) as a follows:

$$ln\left(\frac{I_0}{T^2}\right) - \frac{1}{2}\left(\frac{q\sigma_{so}}{kT}\right)^2 = ln(AA^*) - \frac{q\overline{\Phi}_{Bo}}{kT} \quad (11)$$

The adjusted or modified Richardson plots (Eq. (11)) for LBR and MBR were drawn and shown in Fig. 10(a, b), respectively. As seen in Fig. 10(a) and (b), these plots have also two good linear parts with different slopes. These two linear regions are corresponding to LTR (100–200 K) and HTR (220–320 K), respectively.

Thus, the mean value of $\overline{\Phi}_{Bo}$ and effective Richardson constant (A^*) both for LBR and MBR were obtained from the slopes and interceptions of the Fig. 10(a) and (b) for both LTR and HTR. These values for LBR were found as 0.730 eV, 114.12 A cm^{-2} K^{-2} for LTR and 1.304 eV, 97.33 A cm^{-2} K^{-2}, respectively. Similarly, for MBR these values were also found as 0.687 eV, 144.97 A cm^{-2} K^{-2} for LTR and 1.165 eV, 122.11 A cm^{-2} K^{-2} for HTR, respectively. As conclusion, all of these Figs. 7–10 show a distinctive two linear parts with different slopes in the both LBR and MBR regions, respectively. These experimental results are an evidence to the presence of double GD of BHs in the Au/(0.07Zn-PVA)/n-4H-SiC (MPS) type SD. However, the obtained experimental values of $\overline{\Phi}_{Bo}$ from Figs. 7, 8 and 10 are in good agreement each other for the LBR and MBR. But, for HTR the value of mean BH is higher compared with those in LTR due to the voltage dependent of BH and *n*. The large deviation between the experimental and theoretical values of the A^* was attributed to the fact that the temperature-dependent *I-V* characteristics are used for calculation. However, it may be affected by the lateral inhomogeneity of the BH and potential fluctuations at the Schottky interface [8–18,59]. As a result, the current-transport or conduction in the Au/(0.07Zn- PVA)/n-4H-SiC (MPS) SD can be successfully explained by of TE mechanism with the double GD of BHs.

4. Conclusion

Au/(0.07Zn-PVA)/n-4H-SiC (MPS) type SDs were fabricated and

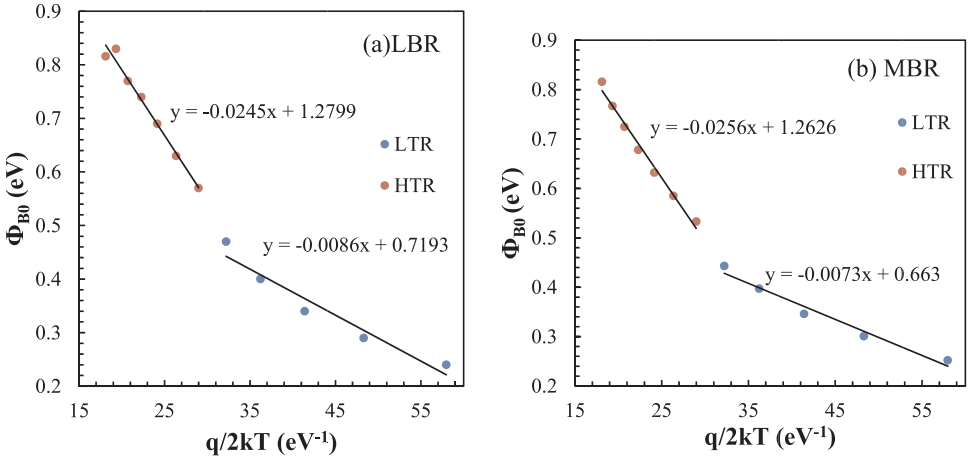

Fig. 8. Φ_{B0} vs $q/2kT$ plots for Au/(0.07Zn-PVA)/n-4H-SiC SD for (a) LBR and (b) MBR.

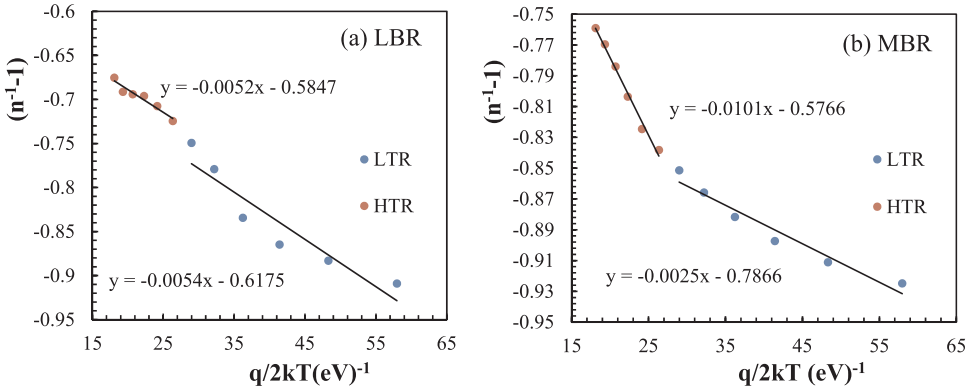

Fig. 9. $(n^{-1} - 1)$vs $q/2kT$ plots for Au/(0.07Zn-PVA)/n-4H-SiC SD for (a) LBR and (b) MBR.

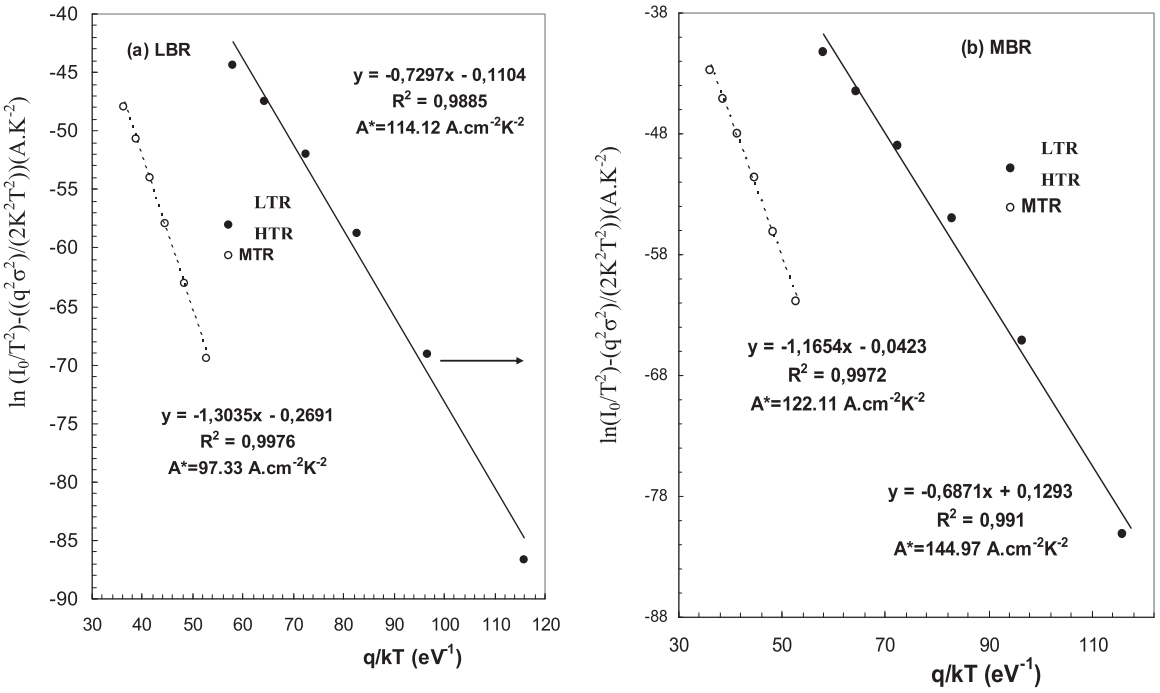

Fig. 10. The modified Richardson plots for Au/(0.07Zn-PVA)/n-4H-SiC (MPS) SD for (a) LBR and (b) MBR, respectively.

their current-conduction/transport were investigated in the wide range of temperature (100–320 K) to get more information on the formation of BH at Au/(n-4H-SiC) interface and possible conductions mechanisms. The semi-logarithmic forward bias *I-V* plots showed two distinctive linear parts/regions which correspond to low and intermediate/moderate bias regions, LBR and MBR, respectively. The obtained experimental values of n and Φ_{B0} exhibited a strong dependence of temperature. These values were found as 10.99 and 0.240 eV (at 100 K) and 3.08 and 0.0.830 eV (at 320 K) for the LBR, respectively. On the other hand, they were obtained as 13.31 and 0.252 eV (at 100 K) and 4.15 and 0.767 eV (at 320 K), respectively, for MBR. It is clear that the value of n decreases with increasing temperature, but Φ_{B0} increases. The observed constant values of (nkT/q) for MBR is the result of tunneling mechanism which is including thermionic field emission (TFE) and FE theories and these mechanisms may be the dominant ones especially at low temperatures. The obtained high value of n even at room temperature cannot be explained by the existence of an interfacial layer, surface states, TFE and FE theories. However, such high values of n also indicated that the existence of a non-uniform distribution of BH at the M/S interface where charge-transport across the BH may be described by considering a Gaussian distribution of BHs at around mean value of it. For this purpose, the Φ_{B0} vs n, Φ_{B0} vs $q/2kT$ and $(n^{-1} - 1)$ vs $q/2kT$ plots were drawn to get proof for the GD of BH. All these figures also revealed two distinctive linear parts with different slopes which are called as LTR (100–200 K) and HTR (220–320 K), respectively. In this way, the classic Richardson plot was modified by using the obtained values of σ_{so} from Φ_{B0} vs $q/2kT$ plots for two bias regions. Thus both the values of $\overline{\Phi}_{B0}$ and A^* for LBR were found as 0.730 eV, 114.12 A cm^{-2} K^{-2} for LTR ($100 \leq T \leq 200$ K) and 1.304 eV, 97.33 A cm^{-2} K^{-2} for HTR ($200 \leq T \leq 320$ K), respectively, from the slope and intercept of these plots. These values for MBR were also found as 0.687 eV, 144.97 A cm^{-2} K^{-2} for LTR and 1.165 eV, 122.11 A cm^{-2} K^{-2} for HTR, respectively. It is clear that the values of A^* especially for MBR for LTR are very close to the theoretical value of it (146 A cm^{-2} K^{-2}) for n-4H-SiC. In conclusion, the CCM in Au/(0.07Zn-PVA)/n-4H-SiC (MPS) SD can be successfully explained by TE mechanism with the double GD of BHs.

Acknowledgments

This study is supported by Scientific Research Project in Süleyman Demirel University (Project No: 4614-D2-16).

References

[1] S. Demirezen, A. Kaya, Ö. Vural, Ş. Altındal, The effect Mo-doped PVC + TCNQ interfacial layer on the electrical properties of Au/PVC + TCNQ/p-Si structures at room temperature, Mater. Sci. Semicond. Process. 3 (2015) 140–148.

[2] Z. Khurelbaatar, K.H. Shim, J. Cho, H. Hong, V.R. Reddy, C.J. Choi, Temperature dependent current-voltage and capacitance-voltage characteristics of an Au/n-type Si Schottky barrier diode modified using a PEDOT:PSS, Inter. Mater. Trans. 56 (1) (2015) 10–16.

[3] Ş. Altındal Yerişkin, M. Balbaşı, İ. Orak, The effects of (graphene doped PVA) interlayer on the determinative electrical parameters of the Au/n-Sİ (MS) structures at room temperature, J. Mater. Sci.: Mater. Electron. 28 (2017) 14040–14048, http://dx.doi.org/10.1007/s10854-017-7255-1.

[4] K. Moraki, S. Bengi, S. Zeyrek, M.M. Bülbül, Ş. Altindal, Temperature dependence of characteristic parameters of the Au/$C_{20}H_{12}$/n-Si Schottky barrier diodes (SBDs) in the wide temperature range, J. Mater Sci: Mater Electron. 〈http://dx.doi.org/10.1007/s10854-016-6011-2〉.

[5] O. Çiçek, H.U. Tecimer, S.O. Tan, H. Tecimer, I. Orak, Ş. Altindal, Synthesis and characterization of pure and graphene (Gr)-doped organic/polymer nanocomposites to investigate the electrical and photoconductivity properties of Au/n-GaAs structures, Compos. Part B 113 (2017) 14–23.

[6] H. Tecimer, T. Tunç, Ş. Altındal, Investigation of photovoltaic effect on electric and dielectric properties of Au/n-Si Schottky barrier diodes with nickel (Ni)–zinc (Zn) doped organic interface layer, J. Mater. Sci: Mater. Electron. 〈http://dx.doi.org/10.1007/s10854-017-8314-3〉.

[7] J.P. Sullivan, R.T. Tung, M.R. Pinto, W.R. Graham, Electron transport of inhomogeneous Schottky barriers: a numerical study, J. Appl. Phys. 70 (1991) 7403.

[8] W. Mönch, Barrier heights of real Schottky contacts explained by metal-induced gap states and lateral inhomogeneities, J. Vac. Sci. Technol. B 17 (1999) 1867.

[9] S. Chand, J. Kumar, Evidence for the double distribution of barrier heights in Pd_2Si/n-Si Schottky diodes from I-V-T measurements, Semicond. Sci. Technol. 11 (1996) 1203.

[10] S. Chand, J. Kumar, Electron transport and barrier inhomogeneities in palladium silicide Schottky diodes, Appl. Phys. A 65 (1997) 497–503.

[11] A. Gümüş, A. Türüt, N. Yalçın, Temperature dependent barrier characteristics of CrNiCo alloy Schottky contacts on n-type molecular-beam epitaxy GaAs, J. Appl. Phys. 91 (2002) 245.

[12] R.T. Tung, Electron transport at metal-semiconductor interfaces: general theory, Phys. Rev. B 45 (1992) 13509.

[13] Y.P. Song, R.L. Van Meirhaeghe, R.L. Laflere, F. Cordon, On the difference in apparent barrier height as obtained from capacitance–voltage and current–voltage temperature measurements on Al/p-InP Schottky barriers, Solid State Electron. 29 (1986) 633–638.

[14] J.H. Werner, H.H. Guttler, Barrier inhomogeneities at Schottky contacts, J. Appl. Phys. 69 (1991) 1522.

[15] J. Osvald, Z.J. Horvarth, Theoretical study of the temperature dependence of electrical characteristics of Schottky diodes with an inverse near-surface layer, Appl. Surf. Sci. 234 (2004) 349–354.

[16] Z.J. Horvarth, Comment on, analysis of I-V measurements on $CrSi_2$Si Schottky structures in a wide temperature range, Solid State Electron. 39 (1996) 176–178.

[17] S. Alialy, Ş. Altındal, E.E. Tanrıkulu, D.E. Yıldız, Analysis of temperature dependent current-conduction mechanisms in Au/TiO_2/n-4H-SiC (metal/insulator/semiconductor) type Schottky barrier diodes, J. Appl. Phys. 116 (2014) 083709.

[18] T. Kimoto, J.A. Cooper, Fundamentals of Silicon Carbide Technology, 1st ed., John Wiley & Sons, Singapore, 2014.

[19] O. Kamoun, A. Boukhachem, A. Yumak, P. Petkova, K. Boubaker, M. Amlouk, Europium incorporation dynamics and some physical investigations within ZnO sprayed thin films, Mater. Sci. Semicond. Process. 43 (2016) 8.

[20] P.K. Singh, M.S. Gaur, R.S. Chauhan, Dielectric properties of sol–gel synthesized polysulfone–ZnO nanocomposites, J. Therm. Anal. Calorim. 122 (2015) 725.

[21] I. Yücedağ, A. Kaya, H. Tecimer, Ş. Altındal, Temperature and voltage dependences of dielectric properties and ac electrical conductivity in Au/PVC + TCNQ/p-Si structures, Mater. Sci. Semicond. Process. 28 (2014) 37.

[22] M. Sharma, S.K. Tripathi, Analysis of interface states and series resistance for Al/PVA: n-cds nanocomposite metal–semiconductor and metal–insulator–semiconductor diode structures, Appl. Phys. A 113 (2013) 491.

[23] H. Tecimer, H. Uslu, Z.A. ALahmed, F. Yakuphanoglu, Ş. Altındal, On the frequency and voltage dependence of admittance characteristics of Al/PTCDA/P-Si (MPS) type Schottky barrier diodes (SBDs), Compos. Part B 57 (2014) 25.

[24] S. Altındal Yeriskin, M. Balbasi, A. Tataroğlu, Frequency and voltage dependence of dielectric properties, complex electric modulus, and electrical conductivity in Au/7% graphene doped-PVA/n-Si (MPS) structures, J. Appl. Polym. Sci. (2016), http://dx.doi.org/10.1002/APP.43827.

[25] U. Aydemir, İ. Taşçıoğlu, Ş. Altındal, İ. Uslu, A detailed comparative study on the main electrical parameters of Au/n-Si and Au/PVA:Zn/n-Si Schottky barrier diodes, Mater. Sci. Semicond. Process. 16 (2013) 1865.

[26] C. Tozlu, A. Mutlu, Poly(melamine-*co*-formaldehyde) methylated effect on the interface states of metal/polymer/p-Si Schottky barrier diode, Synth. Met. 211 (2016) 99.

[27] H. Tecimer, A. Turut, H. Uslu, Ş. Altındal, İ. Uslu, Temperature dependent current-transport mechanism in Au/(Zn-doped)PVA/n-GaAs Schottky barrier diodes (SBDs), Sens. Actuators A 199 (2013) 194.

[28] M. Sharma, S.K. Tripathi, Temperature dependent current-voltage (IV) characteristics of Al/n-cadmium selenide-polyvinyl alcohol (Al/n-CdSe-PVA) Schottky diode, Optoelectron. Adv. Mater. 6 (1–2) (2012) 200–204.

[29] T. Tunc¸, I. Uslu, I. Dokme, Ş. Altindal, H. Uslu, Frequency and temperature dependence of dielectric properties of Au/polyvinyl alcohol (Co, Ni-Doped)/n-Si Schottky diodes, Int. J. Polym. Mater. 59 (2010) 739.

[30] P. Fatehi, H. Xiao, Effect of cationic PVA characteristics on fiber and paper properties at saturation level of polymer adsorption, Carbohydr. Polym. 79 (2010) 423.

[31] Wankei Wan, A. Dawn Bannerman, Lifang Yang, Helium Ma, Poly(Vinyl Alcohol) cryogels for biomedical applications, Polym. Cryogels Adv. Polym. Sci. 263 (2014) 7–8.

[32] U. Thanganathan, J. Parrondo, B. Rambabu, Nanocomposite hybrid membranes containing polyvinyl alcohol or poly(tetramethylene oxide) for fuel cell applications, J. Appl. Electrochem. 41 (2011) 617.

[33] İ. Uslu, B. Baser, A. Yaylı, M.L. Aksu, Preparation and characterization of PVA/Zinc acetate/boron composite fibers, e-Polymers 145 (2007).

[34] İ. Uslu, H. Dastan, A. Altas, A. Yaylı, O. Atakol, M.L. Aksu, Preparation and characterization of PVA/boron polymer produced by an electrospinning technique, e-Polymers 133 (2007).

[35] H. Satio, B. Stuhn, Dielectric study of the crystal-amorphous interphase in poly (vinylidene fluoride)/poly(methyl methacrylate) blends, Polymer 35 (1994) 475.

[36] H. Pan, L.M. Li, L. Hu, X.J. Cui, Continuous aligned polymer fibers produced by a modified electrospinning method, Polymer 47 (2006) 4901.

[37] V.R. Reddy, V. Manjunath, V. Janardhanam, C.H. Leem, C.J. Choi, Double Gaussian distribution of barrier heights, interface states, and current transport mechanisms in Au/$Bi_{0.5}Na_{0.5}TiO_3$-$BaTiO_3$/n-GaN MIS structure, J. Electron. Mater. 44 (2015) 549–557.

[38] Ç.Ş. Güçlü, A.F. Özdemir, Ş. Altındal, Double exponential I–V characteristics and double Gaussian distribution of barrier heights in (Au/Ti)/Al_2O_3/n-GaAs (MIS)-type Schottky barrier diodes in wide temperature range, Appl. Phys. A 122 (2016) 1032.

[39] V. Rajagopal Reddy, Electrical properties of Au/poly vinylidene fluoride/n-InP Schottky diode with polymer interlayer, Thin Solid Films 556 (2014) 300.

[40] E. Marıl, A. Kaya, H.G. Çetinkaya, S. Koçyiğit, Ş. Altındal, On the temperature dependent forward bias current–voltage(I–V) characteristics in Au/2% graphene–cobalt doped($Ca_3Co_4Ga_{0.001}O_x$)/n-Si structure, Mater. Sci. Semicond. Process. 39 (2015) 332.

[41] B. Prasanna Lakshmi, M. Siva Pratap Reddy, A. Ashok Kumar, V.R. Reddy, Electrical transport properties of Au/SiO2/n-GaN MIS structure in a wide temperature range, Curr. Appl. Phys. 12 (2012) 765.

[42] E. Marıl, A. Kaya, S. Koçyiğit, S. Altındal, On the analysis of the leakage current in Au/Ca3Co4Ga0.001Ox/n-Si structure in the temperature range of 80–340 K, Mater. Sci. Semicond. Process. 31 (2015) 256.

[43] A. Kumar, S. Vinayak, R. Singh, Micro-structural and temperature dependent electrical characterization of Ni/GaN Schottky barrier diodes, Curr. Appl. Phys. 13 (2013) 1137.

[44] S. Altındal, Yerişkin, M. Balbaşı, S. Demirezen, Temperature and voltage dependence of barrier height and ideality factor in Au/0.07 graphene-doped PVA/n-Si structures, Indian J. Phys. 91 (2017) 421–430.

[45] S. Alialy, A. Kaya, E. Marıl, S. Altındal, I. Uslu, Electronic transport of Au//n-Si structures analysed over a wide temperature range, Philos. Mag. 95 (2015) 1448–1461.

[46] H. Tecimer, S. Aksu, H. Uslu, Y. Atasoy, E. Bacaksız, Ş. Altındal, Schottky diode properties of $CuInSe_2$ films prepared by a two-step growth technique, Sens. Actuators A 185 (2012) 73.

[47] Zs.J. Horvarth, Comment on "Analysis of I-V measurements on $CrSi_2$-Si Schottky structures in a wide temperature range", Solid-State Electron. 39 (1996) 176.

[48] A. Sarıyıldız, Ö. Vural, M. Evecen, Ş. Altındal, Single Gaussian distribution of barrier height in Al/PS–ZnPc/p-Si type Schottky barrier diode in temperature range of 120–320 K, J. Mater. Sci: Mater. Electron. 25 (2014) 4391–4397.

[49] R.F. Schmitsdrof, T.U. Kampen, W. Mönch, Explanation of the linear correlation between barrier heights and ideality factors of real metal-semiconductor contacts by laterally nonuniform Schottky barriers, J. Vac. Sci. Technol. B 15 (1997) 1221.

[50] J.H. Werner, H.H. Güttler, Barrier inhomogeneities at Schottky contacts, J. Appl. Phys. 69 (1991) 1522.

[51] M.S.P. Reddy, H.S. Kang, J.H. Lee, V.R. Reddy, J.S. Jang, Electrical properties and the role of inhomogeneities at the polyvinyl alcohol/n-InP Schottky barrier interface, J. Appl. Polym. Sci. 131 (2014) 39773.

[52] E.H. Rhoderick, Metal-Semiconductor Contacts, Oxford University Press, 1978.

[53] H.E. Lapa, A. Kökce, M. Al-Dharob, İ. Orak, A.F. Özdemir, Ş. Altındal, Interfacial layer thickness dependent electrical characteristics of Au/(Zn-Doped PVA)/n-4H-SiC (MPS) structures at room temperature, Eur. Phys. J. Appl. Phys. 80 (2017) 10101.

[54] S.M. Sze Kwok, K. Ng, Physics of Semiconductor Devices, Third ed., John Wiley & Sons, Inc, Hoboken, New Jersey, 2007.

[55] E.H. Nicollian, J.R. Brews, MOS Physics and Technology, Wiley, New York, 1982.

[56] C.R. Crowell, V.L. Rideout, Normalized thermionic-field (T-F) emission in metal-semiconductor (Schottky) barriers, Solid-State Electron. 12 (1969) 89.

[57] F.A. Padovani, R. Stratton, Field and thermionic-field emission in Schottky barriers, Solid-State Electron. 9 (1966) 695.

[58] Z.J. Horvath, Comment on analysis of I-V measurements on $CrSi_2$/Si Schottky structure in a wide temperature range, Solid-State Electron. 39 (1996) 176–178.

[59] S. Chand, J. Kumar, Effects of barrier height distribution on the behavior of a Schottky diode, J. Appl. Phys. 82 (1997) 5005–5010.